Precise electrical determination of the field- and current-induced switching mode of a magnetic nanodisk in a non-local spin valve

R. M. Reeve, A. Pfeiffer, and M. Kläui*
Institut für Physik, Johannes Gutenberg-Universität Mainz, 55099 Mainz, Germany and Graduate School of Excellence Materials Science in Mainz (MAINZ), Staudinger Weg 9, 55128 Mainz, Deutschland

G. Zhand, J. P. Attané, and L. Vila
University Grenoble Alpes, CEA, CNRS, Spintec, F-38000 Grenoble, France
(Dated: May 31, 2021)

In this work, we study the manipulation and the detection of the magnetic state and switching modes of a Permalloy disk, using a non-local spin-valve with dual CoFe injectors and with the disk acting as the detector electrode. Applying simultaneously external magnetic fields and spin currents from the injectors, we demonstrate the possibility to use the spin torque created by the spin current to modulate the switching modes and switching fields of the disk, following the disentanglement of the influence of Joule heating. Moreover, by engineering the device to have a very small overlap of the spin conduit with one side of the disk, we demonstrate how, with the help of a first-order reversal curve analysis, we can extract the precise details of the switching from the monodomain to the vortex state, including the chirality of the system without the need for direct imaging.

I. INTRODUCTION

Thin magnetic nanodisks are attractive systems for fundamental research studies and are exciting candidates for various spintronic applications.[1–5] For small enough systems, such disks exhibit two main magnetic states; the quasi-uniform state, which is energetically preferred for low diameters and thicknesses of the disk, and the vortex state, which is stable for larger thicknesses and diameters.[6–10] Depending on the history of the system, there is a large range of disk sizes for which both states can be metastable, and in large systems a multiplicity of other configurations can also be found.[11] The vortex state is characterized by an in-plane curling of the magnetization around an out-of-plane magnetized vortex core region.[12,13] The sense of rotation is termed the chirality, c, with c being defined as $c = \pm 1$ for the anticlockwise and clockwise case, while the out-of-plane direction of the vortex core is termed the polarity and given by $p = \pm 1$ for an up or down orientation, respectively. The vortex state is of particular fundamental interest due to its special topological properties and rich dynamics.[14,15] Additionally, due to the high stability and inherent low stray field from the vortex state, it has been proposed as a promising system for high density magnetic memories that employ the different configurations to store data,[1–3] while the gyrational dynamics of the state make it attractive for RF oscillators.[4] A nanodisk has also recently been used as a tunable spin-absorber in a non-local spin-valve type structure which could be employed for spin-transistor type devices.[16] Furthermore, arrays and chains of disks have been investigated as interesting systems for magnonic vortex crystals[17] and magnetic logic mediated via the stray field coupling of the vortex cores.[5]

In addition to the stability of the different states, the switching of nanoscale magnetic disks between the quasi-uniform state and the vortex state has been investigated. In many studies, such a switching mode is inferred from hysteresis measurements using the magneto-optical Kerr effect or superconducting quantum interference device magnetometry,[6,7,18,19] with supporting details of the switching mechanisms provided via micromagnetic simulations.[18,20] Again, depending on the size of the system, different switching modes are deduced from the

hysteresis loops, including for the smallest disks switching from the monodomain state to the reverse monodomain state in a single-step via coherent rotation of the magnetization, or for slightly larger systems a two step switching process which occurs via the initial nucleation of the vortex state and the subsequent expulsion of the vortex core at high reverse fields to yield the reverse monodomain state.[20] Many of these experimental techniques, however, tend to average over a large array of disks, yielding switching properties that are an average of the behaviour of the ensemble.

Electrical measurements, conversely, are a convenient, device-relevant and widely available approach to detect the switching of individual nanostructures via the different anisotropic magnetoresistance signals of different spin configurations and their dynamics.[21–25] Here, however, the signal is averaged over the whole current path through the disk, which makes it challenging to interpret the results[23] and to determine precise details of a given state, such as the chirality of the vortex state and the region of vortex core nucleation and annihilation in the disk during the switching, a property which can be strongly influenced by defects and inhomogeneities in a real experimental system. Approaches to partially overcome this have included the use of multiple electrical contacts to the disk in order to confine the current path,[24] which is however difficult to apply in the case of very small disks. Furthermore, more advanced electrical detection schemes have been devised based on the different dynamic response of the various vortex configurations, which can provide details concerning the state polarity and chirality,[25–29] however these are more difficult to apply in a device and also average over the current path in the structure.

For detecting the precise details of the switching and dynamics of individual nanoscale magnetic systems, including magnetic disks, the method of choice is usually high-resolution magnetic imaging. Techniques include soft x-ray microscopy[17,30] or scanning electron microscopy with polarization analysis,[31] which, however, are not widely available, or magnetic force microscopy[32] which is more widely available but where image acquisition is slow. Furthermore such techniques are not suitable for detecting the state of a system in a device context. Hence for both fundamental studies and for devices it would be desirable to have an easy approach for the electrical detection of the vortex state chirality and the details of the disk switching, as well as efficient means to electrically control the state.

One attractive approach to the electrical switching and detection of magnetic states is the non-local spin-valve geometry, where pure spin currents are employed to manipulate and sense a magnetic state. In such a geometry, a pure spin current is generated in a non-magnetic spin conduit, most typically via spin-injection from a ferromagnetic electrode,[33–36] although other pure spin current generation mechanisms have also been employed.[37–39] The spin current then diffuses along the conduit without an accompanying net charge current, and is subsequently detected at a ferromagnetic detector electrode as a non-local voltage. The size of the signal depends on the magnitude of the spin current as well as the relative alignment of the spin current and magnetization at the precise position where the spin current is absorbed by the local magnetization. Such a device has been proposed as an exciting candidate for next-generation readheads for high storage density media.[40,41] Furthermore, the absorption of the spin current can be employed to exert a torque on the magnetization in order to manipulate the magnetic state of the detector.[42,43] In this manner it has been shown that it is possible to switch magnetic nanomagnets[44,45] and manipulate magnetic domain walls with high efficiency,[46–48] while reducing some of the potentially unwanted contributions from the charge current such as Oersted fields and Joule heating in the region where the magnetization is being manipulated. Of particular interest for the detection of magnetic states is the fact that the detected voltage probes a region of absorption at the conduit-detector interface[47] and hence it can be used as a very precise probe of the magnetic state from that particular area of the system. This has, for example, been

employed to detect details of magnetic domain wall motion even underneath the spin current conduit.[47] Such non-local spin valves could also be a powerful tool to manipulate and detect the different states of thin disks and provide a simple electrical means to detect the chirality of the vortex state[49] and in particular details of the switching. For a full understanding of the electrical control and detection of the vortex state, simultaneous measurements of the spin current detection and spin current assisted manipulation of the state in a single device are needed including the determination of the details of the switching modes, calling for a detailed study as we perform here.

In this work we investigate the switching of a Permalloy (Py) disk by fields and pure spin currents in a dual-injector non-local spin valve device. We generate pure spin currents via electrical injection from two tilted CoFe injector electrodes. The spin currents are then employed to assist in the switching of a nanoscale magnetic disk and are shown to have a measurable effect in modifying the switching behaviour of the system despite their very localized region of action. We show how the non-local detection scheme provides a very sensitive electrical probe of the switching behaviour of the system which allows us to determine the details of the switching modes, and the state chirality and stability, as confirmed via first order reversal curve measurements.

II. METHODS

Non-local spin valves with dual angled injectors and a disk as the detector[50] have been fabricated, as shown in Figure 1. CoFe ($Co_{60}Fe_{40}$) has been chosen for the injectors due to the large reported spin signals arising from the high effective polarization of the material[51] and the high coercivity which prevents the electrodes from being switched for low applied fields, while Py ($Ni_{80}Fe_{20}$) has been selected for the disk due to the soft magnetic properties and low intrinsic anisotropy. The disk is nominally patterned to be circular, however a small degree of ellipticity may arise from the fabrication process. The diameter of the uncovered part of the disk is 160 nm and its thickness is 10 nm so that both the quasi-uniform state and the vortex state are expected to be metastable.[6] The non-magnetic conduit has a width of 70 nm and has been fabricated from 80 nm thick Cu, along with the electrical contacts. The CoFe wires have a thickness of 30 nm and are 70 nm wide. The structures have been produced in a standard three step electron beam lithography process, followed by a lift-off procedure, with the different materials at each stage being deposited by ultra-high vacuum evaporation. The samples have been characterized via a standard non-local detection approach.[47,52] The full electrical setup for the measurements is shown in Figure 1. The dual CoFe electrode geometry allows for the injection of spin currents from the individual electrodes or additionally the simultaneous injection from both sides of the disk. Current pulses for assisting the switching of the disk are provided via pulse generators that inject currents from the injectors into the copper spin conduit via the left (contacts 1-2) or right (contacts 5-6) CoFe wire. The transmitted pulses are detected using an oscilloscope and from these, the applied charge current density is calculated. The state of the disk is detected via measurement of the non-local voltage signal (V_{NL}) for the disk employed as the detector electrode (contacts 4-3), following the injection of a small probe current of 85 μA at a frequency of 2221 Hz in the left injector (contacts 1-2). This can then be converted to a non-local resistance R_{NL} based on the size of the probe current. To account for slight differences in the resistance of the two CoFe wires, a 10 kΩ pre-resistor is used before the sample in certain measurements to provide a constant current source. Pick-off Ts are employed to disentangle the low frequency, low amplitude lock-in excitation from the high frequency, high amplitude current pulses. By careful impedance matching and the employment of suitable attenuators (as indicated in the figure), significant reflections of the current pulses back to the sample are suppressed. Measurements have been performed in a bath cryostat at a

cryostat temperature of 4.2 K. The cryostat is equipped with a Helmholtz coil for the application of very precise 2D vector fields within the plane of the sample. The coordinate system for the field with respect to the sample is indicated in the top left of Figure 1. We measure the non-local signal at the disk detector electrode as a function of the applied field magnitude and direction, for different magnitudes of the injected spin current from current pulse injection in either the left, or right electrode, or with simultaneous injection from both electrodes. Since the maximum applied fields in these measurements of 120 mT are too small to switch the state of the hard-magnetic CoFe injector electrodes, as confirmed by our data, the non-local signal is a measure of the magnetic state of the disk detector. For field-induced switching of the disk, measurements are performed by incrementally increasing the magnetic field along a chosen axis and detecting the non-local signal for each field-step, with the other connections kept at high-impedance. In the case of spin-current assisted switching, 10 μs long current pulses are applied at each field stage in either or both CoFe injectors via the two synchronized pulse generators. Complementary characterization of the system is also provided via an angle-sweep measurement, where the magnitude of the field is kept constant at 120 mT and the angle of the field is incrementally rotated while detecting the non-local signal.

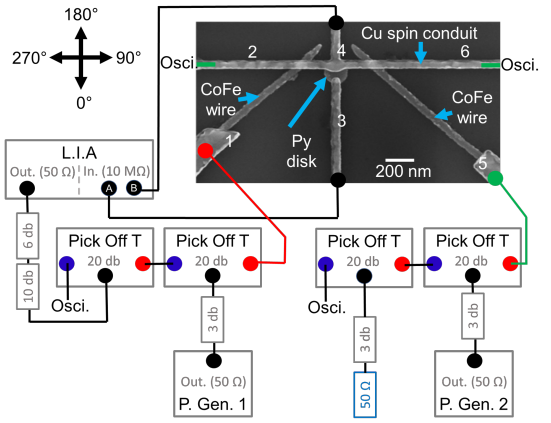

FIG. 1. Schematic of the employed experimental setup, overlayed on a scanning electron microscope image of the sample. Pulse generators (P. Gen.) provide current pulses to the injectors (i.e. the CoFe wires), generating a spin current in the copper conduit via spin injection. The current pulses are measured with an oscilloscope (Osci.). The state of the disk is detected via a non-local measurement by use of a lock-in amplifier (L.I.A), following injection of a small probe current from the left CoFe ($Co_{60}Fe_{40}$) wire to the Cu spin conduit (contacts 1-2). Pick-off Ts are employed to disentangle the high-frequency excitation current pulses and the low-frequency lock-in probe currents. The employed attenuators and terminations are indicated by the small rectangles. The angular coordinate system for the externally applied magnetic field is displayed in the upper left corner.

III. RESULTS

We first present the angular dependence of the non-local signal, as seen in Figure 2. Panel (a) shows the signal for current injection in the left electrode, while panel (b) shows the signal for current injection in the right electrode. In both cases a roughly sinusoidal signal is seen, with a different phase offset in each case. The sinusoidal behaviour arises from the fact that the magnetization of the injector is expected to remain fixed for given applied fields, only exhibiting a small canting away from the geometrically defined easy-axis along the wire. If this were not the case we would expect to see sharp jumps in the signal corresponding to the switching of the injectors, which is clearly not observed. As a result, to a good approximation, the signal therefore directly represents the orientation of the disk magnetization in the region where the spin current is absorbed below the contact. Since the spin diffusion length in Py is only a few nm,[53] the region that dominates the signal is very localized and hence precise details of the spin structure in the contact area can be determined. This finding is important, as it allows for the detection of particular signatures of the switching mechanism in the disk, as presented below. In this measurement, the field

is sufficient to largely saturate the Py detector due to its soft magnetic properties, and hence the magnetization of the disk (and correspondingly the detected signal) gradually rotates with the field. From the maxima in the two signals we can determine the orientation of the magnetization of the two injector electrodes. Since the non-local signal is maximum for a parallel alignment of the detector and injector, we find that the left injector is oriented along the 135° direction, while the right electrode is aligned along 45°, consistent with the design in Fig. 1. Additionally it can be noted that the signal amplitude from the left injector is significantly larger than that for the right injector. While a certain difference in signal amplitude could be accounted for by the non-local signals being dominated by a region of hotspot absorption that is located on the left side of the disk, this does not explain the magnitude of the observed effect. More likely is a lower spin transmittivity of the right injector-conduit interface due to the presence of defects,[52] resulting in a lower effective spin polarization of the injected spin current from this side. As a result of this we mainly use the left injector electrode for the injection of current pulses and the generation of the non-local signal, while in certain measurements we additionally use the right electrode to provide further current pulses and larger total spin currents than are possible from just one electrode alone, as described in the relevant cases.

Next we look at the details of the switching of the disk and the influence of a spin current assisting the switching via hysteresis measurements. Figure 3 shows the switching behaviour of the system, as detected via the non-local signal, for 4 selected angles of the field; 165/345°, 0/180°, 90/270° and 351/171°, presented in panels (a-d), respectively. The field orientation is indicated by the brown arrows on the axes to the side, along with the injected spin polarization P, which is aligned with the magnetization of the injector, M_{Inj}. As discussed in detail later, the non-local signal then probes the relative angle between M_{Inj} and the magnetization of the disk under the contact (shown as $M_{1,2}$ for particular points indicated on the

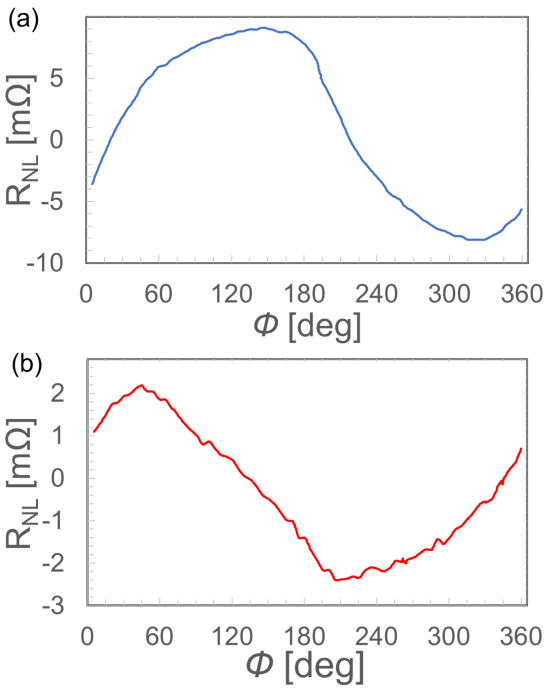

FIG. 2. Non-local signals as a function of the applied field angle for a fixed field amplitude of 120 mT. a) Current injection in the left CoFe injector (contacts 1-2). b) Current injection in the right CoFe injector (contacts 5-6).

hysteresis loops) and hence this hysteresis reveals quantitative details of the switching of the disk. Column (i) presents the loops in the case of switching by magnetic fields alone. What is immediately apparent is that the loops look very different for the different angles. In particular there are different numbers of steps in the switching process for both the different angles and for positive and negative fields. In (a), (b) and (d) we see various multi-step switching behaviours, whereas in (c) we see that there is a single step switching. While we do additionally observe some stochastic behaviour with slight variations in the switching loops and switching fields for repeated experimental runs, which reveals a small influence of thermally activated processes, for the shown field angles the presented loops are representatitive of the general

shape of the hysteresis curves and the switching behaviour is robustly reproducible for a large proportion of the measurements. The single-step switching is indicative of switching from the monodomain to the reverse-monodomain state, whereas the multi-step switching indicates a more-complicated switching mode such as the nucleation and annihilation of the vortex state as the disk switches. We analyse the details of the shape of the curves and the associated switching modes in sections IV B and IV C.

The influence of a pure spin current in assisting the switching is shown in Figure 3 column (ii), for the same field angles. For these measurements positive current pulses of density 7.6×10^{11} Am^{-2} are applied in the left electrode, leading to a pure spin current in the spin conduit that diffuses to the disk and potentially assists the field switching. It can be seen that the additional application of the current has a strong influence on the shape of the switching curves and in particular modifies the switching fields for the various transitions, in most cases reducing the field required. While this suggests a contribution of the torque from the pure spin current in assisting the switching, it is possible that other effects from the charge current in the injector also play a role, such as Joule heating of the device leading to increased thermal activation. Therefore, in order to disentangle these different potential effects, we focus on a single field direction, 351/171°, for which the observed states are particularly stable and reproducible, and we measure the switching as a function of the assisting current density for different polarity pulses in the injector. The influence of Joule heating can be ascertained by comparing the change in switching fields with current for positive and negative pulses in the injector, since on reversing the direction of the pulses the polarization of the spin current is reversed while the Joule heating remains the same. In Figure 4 we see this comparison for the case of pulses in both injectors individually, as well as simultaneous injection from both injectors, as shown in (i), (ii) and (iii), respectively. Due to the determined orientation of the magnetization in the two injectors we apply positive pulses in one injector and negative pulses in the second injector. The left plots present the evolution for one of the first, low-field jumps, corresponding to the change in state away from the saturated state, while the right plots present the final high-field jump, representing the return to the reverse-saturated state. In all of the graphs the trend for the switching fields is to reduce with increased current density, regardless of the polarity of the current pulses. This effect can therefore be attributed to a predominant influence of Joule heating, which via thermal activation can promote the nucleation and expulsion of the non-uniform spin state. For the first jump the injection of pulses in either of the electrodes individually does not show any dependence on the current polarity, indicating negligible contribution from the spin transfer torque. However for simultaneous injection from both sides the data suggest a small influence of the spin transfer torque from the pure spin current, with the curves diverging for the highest applied current densitites. Similarly for the second jump there is little difference between the curves for single current pulse injection from just one of the injectors, however simultaneous current injection reveals lower switching fields for one set of pulse polarities, again consistent with a small but measurable influence of the spin transfer torque. While the vertical current flowing between the injectors and the conduit will in principle also generate a very small in-plane Oersted field,[48] in the case of simultaneous current pulses in both injectors when we see the largest difference in the plots, any net field at the central position will be lowest due to the opposite polarity of the current in the two injectors and hence this does not explain the results we observe.

IV. DISCUSSION

A. Pure Spin Current Assisted Switching

The observation of a statistically significant influence of the spin current in assisting the switching of the disk shows the effectiveness

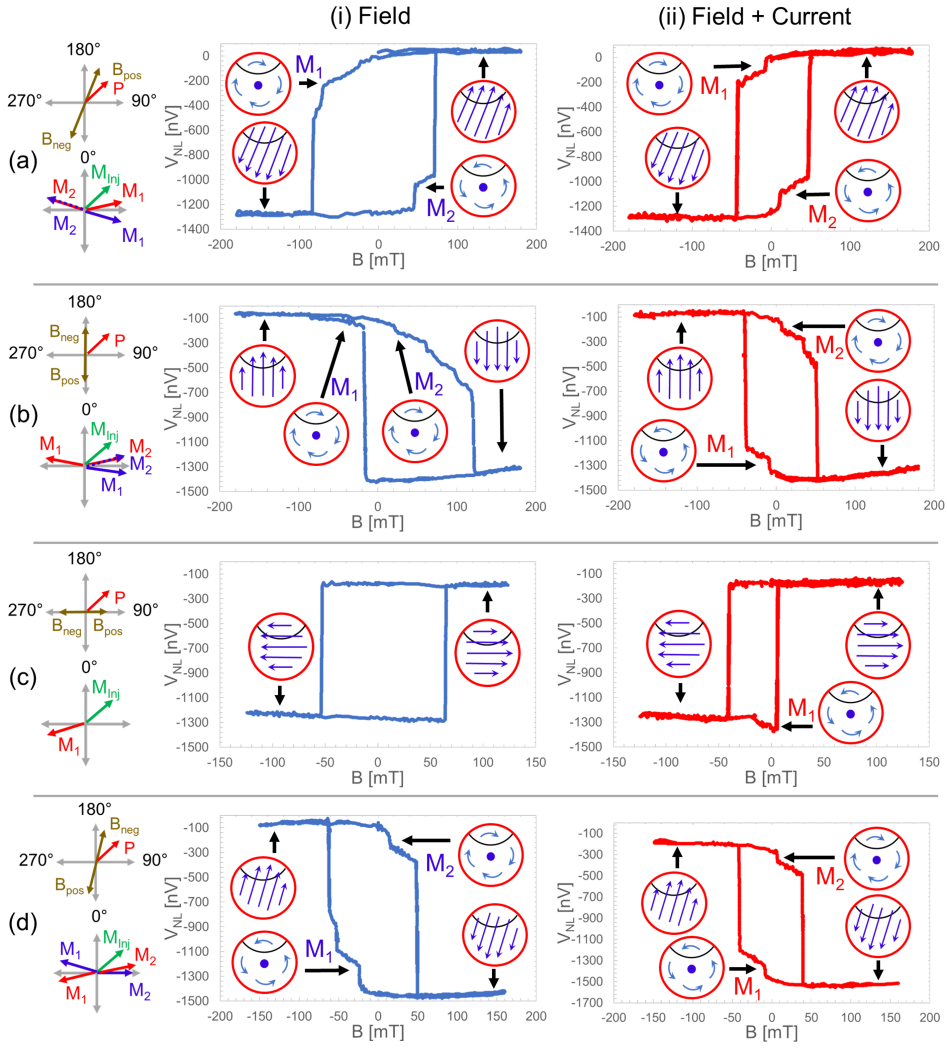

FIG. 3. Non-local signal hysteresis switching loops for field sweeps along (a) 165/345°, (b) 0/180°, (c) 90/270° and (d) 351/171°. (i) shows field induced switching while (ii) shows pure spin current assisted switching for positive current pulses of density 7.6×10^{11} Am^{-2} in the left electrode. The direction of the field ($B_{pos,neg}$) and the spin current polarization (P) is indicated in the upper set of coordinates on the left. The lower coordinates coarsely show the magnetization direction of the disk at the absorption point below the contact for selected stages of the switching process ($M_{1,2}$), as quantitatively calculated from the size of the signal, as well as the direction of the magnetization in the injector, (M_{Inj}). The pictures provide a schematic representation of the inferred magnetic configurations at these points based on the model outlined in section IV, with the black line indicating the contact region where the signal is probed.

of the pure spin currents in a non-local spin valve in modifying the switching pathways. The charge current from the injector generates a pure spin current in the conduit with an effective polarization at the interface on the order of 50%.[51] The spin current diffuses along the

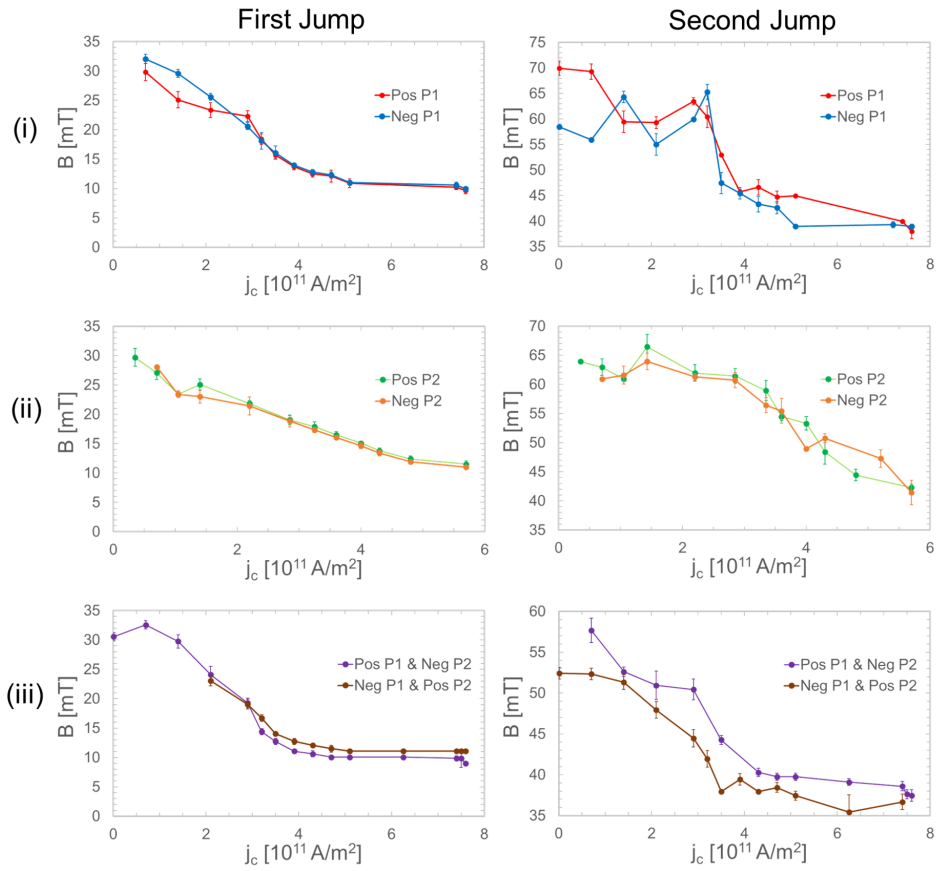

FIG. 4. Dependence of the switching fields on the injector current density for either positive pulses (current applied contacts 1-2 or 5-6) or negative pulses (current applied contacts 2-1 or 6-5) in the different injectors. The field is applied along 351/171° in each case as in Fig. 3 (d). Left plots correspond to the first jump in the signal at negative field, while the right plots correspond to the last jump in the signal at positive field. (i) presents the results for pulses in the left injector (P1), (ii) presents the results for pulses in the right injector (P2) and (iii) presents the results for mixed polarity pulses in the two injectors simultaneously. In this case the currents displayed correspond to the current in the left injector. Due to the slightly different resistances of the two injector electrodes, the current in the second electrode is 25% smaller. The error bars represent the standard error of 4-6 repeated measurement runs. In the cases where all measurements are consistent within 1 mT, no error bar is displayed.

conduit and in a 1-D model decays exponentially due to spin relaxation processes.[51,54–56] Based on this, the injector-disk separation of $\sim 250\,\mathrm{nm}$ and assuming a low temperature spin diffusion length of Cu of around 900 nm,[56] we can calculate the expected spin current arriving at the disk to be $2.9 \times 10^{11}\,\frac{\hbar}{|e|}\,\mathrm{s}^{-1}\,\mathrm{m}^{-2}$ for the largest current densities of $7.6 \times 10^{11}\,\mathrm{Am}^{-2}$. A portion of this spin current is then absorbed by the ferromagnet and as a result of the angular momentum conservation the absorption of the transverse spin current results in a predominantly damping-like spin torque, $\overrightarrow{\tau}$, on the local magnetization of the form:[42,43]

$$\overrightarrow{\tau} \sim -\frac{\hbar}{2e}\left(\overrightarrow{M} \times \overrightarrow{P} \times \overrightarrow{M}\right), \qquad (1)$$

where $\overrightarrow{M}$ is the magnetization in the absorbed region of the disk and $\overrightarrow{P}$ is the polarization direction of the pure spin current, which follows the direction of the injector for positive pulses and is reversed for negative polarity pulses. Since we expect the disk to be in a quasi-uniform state at high fields due to the predominant contribution of the Zeeman energy, the jumps from/to the saturation level can be attributed to the nucleation and annihilation of non-uniform magnetization configurations. It is noteworthy that in the experiment we find that positive polarity pulses in injector 1 and negative polarity pulses in injector 2 promote the nucleation of the non-uniform state (Figure 4 (a,iii)), whereas the opposite polarity pulses and therefore opposite directed torques assist the annihilation of the non-uniform state (Figure 4 (b,iii)). The results show that simultaneous injection of spin currents from both injectors is an effective strategy to assist in the switching of the nanostructure. In addition to potentially providing a larger total spin current amplitude, our geometry additionally ensures that the spin currents have different orientations for the two injectors and therefore regardless of the orientation of the absorbing magnetization in the disk there is the possibility to generate a spin current with a transverse component to the magnetization. This approach could help achieve faster switching by reducing the incubation time as compared to devices where collinear magnetization is used in the electrodes.[57]

In the present device the influence of the spin current is, however, rather modest. We can use the field-current equivalence approach to quantify the influence of the effect of the spin-transfer torque from the difference in the slopes of the curves at high current-density (above $3.5 \times 10^{11}\,\mathrm{Am}^{-2}$), for the case where we see the larger influence of the pure spin current in 4 (right ,iii).[48,58] This yields an efficiency of $(0.14 \pm 1) \times 10^{-15}\ \mathrm{Tm}^2/\mathrm{A}$ for the combined current density, which is relatively low compared to previous studies.[48,58] The large error bar on this value further highlights the small size of the effect, with the torque efficiency harder to extract from the differences in the slopes as compared to the more statistically significant separation between the curves. However, the small influence of the effect is not surprising, since the region of overlap of the spin conduit has intentionally been kept very small. Due to the short spin diffusion length of the absorbed current in the ferromagnet,[53] the torque from the absorbed spin current can only act in a very restricted region of the disk and hence only acts to modify slightly the switching fields. Nevertheless, the sensitivity of the techique allows for the detection of the effect in our dual injector geometry. In a very simple analysis, if we assume a Py spin diffusion length of 4 nm, the spin current only acts on up to $\frac{1}{6}$ of the volume of the disk, if one assumes that the whole of the overlap region of the disk and the conduit contribute equally. In a lower limit if a single hotspot dominates, as seen in some previous studies,[47] the area of absorption could be as low as around $130\,\mathrm{nm}^3$, which is a factor of 1500 smaller than the total volume of the disk where the field can act. Taking into account this difference as well as a non-optimal alignment of the spin-current and magnetization yields a much higher influence of the pure spin current, in line with previous work for domain walls.[48] The exact size of the probed area is expected to depend strongly on the nature and quality of the interface between the Cu and the Py, which strongly influences the spin transport properties.[52] Nevertheless even in the case of ideal interfaces the aforementioned low spin diffusion length of Py means the signal originates only from the direct vicinity of the Cu contact and therefore selectively probes just one side of the disk. We use this to determine the details of the magnetic states in the next section.

B. Determination of States and Switching Modes

We next discuss the determination of the exact magnetic states and the switching modes from a detailed analysis of the switching loops. The difference in switching loops for the different angles reveals an angular dependence of the switching mode and an asymmetry in the system, despite the nominally symmetric geometry. This is likely partly due to the presence of localized defects in the system which can act as nucleation sites or pinning sites for the vortex core of the vortex state. Previous simulations and imaging reveal that nucleation of the vortex state can occur via different modes,[59] however ultimately all these modes involve the nucleation of vortex cores at the sides of the disks, at points on the edges perpendicular to the axis of the applied field.[18,20] Once the state is nucleated, with continued application of the field the vortex core then travels to the opposite side of the disk, where it is annihilated. In a system where both the vortex and quasi-uniform state are metastable, switching via the vortex state can therefore be promoted for certain field angles, depending on the presence and location of defects at the edge of the disk that favour vortex nucleation. Additionally, defects within the centre of the disk can pin the vortex core as it moves across the disk, leading to a multi-step switching process consisting not only of the nucleation and expulsion of the vortex core, but addionally its intermediate depinning from these defects. Hence it can be expected that the switching processes with more than two levels are associated with such processes. However, such a simplified analysis, based solely on the number of jumps in the signal during the switching does not reveal the details of the vortex state, such as its chirality, nor does it reveal the side of the disk where the vortex nucleates/annihilates.

An additional reason for the different shapes of the curves for different angles is the varying field axis. Since the state of the disk is probed at a fixed point in space underneath the contact, while the field angle changes, the different measurements probe different regions of the switching dynamics in the disk. We can take advantage of this localized probe of a small region of the disk to gain additional information concerning the switching in the system, that is not available from a conventional hysteresis measurement that averages over the whole of the device.

Taking advantage of this localized probing of a small region of the disk, we can understand the basic shape of the loops and the size of the jumps in a simplified model based on a few assumptions. The situation is schematically illustrated in Figure 5, for the simple case of the field applied along the 90/270° axis. Based on the known metastable states in the system,[6] for systems that do not switch directly from the monodomain state which due to the Zeeman energy will be stable at high fields (State I) to the reverse monodomain state (III), we assume that the first jump in the signal corresponds to the nucleation of the vortex state and the last jump to its expulsion. For this simple model we neglect the influence of defects such that transitions do not occur gradually but rather at a fixed field, and that further pinning of the system, which can provide more jumps in the signal, does not occur. We assume that the vortex is nucleated for small reverse fields and consider a constant symmetric vortex state at intermediate fields (states II/IV) with a centralized vortex core until the vortex core is expelled, neglecting the distortion of this state at higher fields.

Four cases are shown for the different possible chiralities of the nucleated vortex state for positive and reverse fields, with the different states sketched below. Considering first plot (a), the switch from state I to II is accompanied by only a small change in the signal. This means that the magnetization direction has not changed considerably under the contact and that the nucleated vortex chirality must be clockwise, since this state has little change in the magnetization at the top of the disk where the signal originates, as seen in the sketches. When the state switches to the reverse monodomain state (II-III), however, the magnetization in the relevant

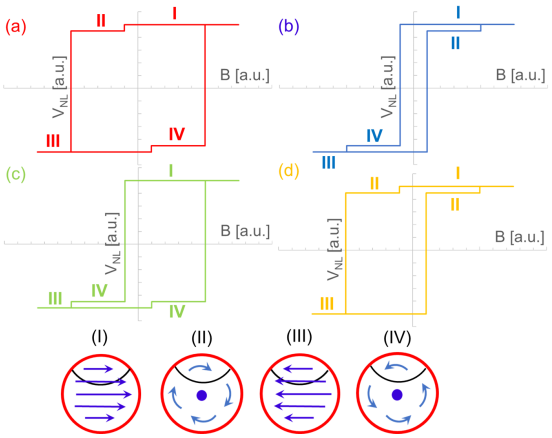

FIG. 5. Simplified model used to qualitatively explain the size of the measured jumps in the nonlocal signal as a result of vortex nucleation and annihilation. Based on whether the small or the large jump is found for small or high external magnetic fields, the chirality of the vortex can be determined. The applied field angle is assumed to be 90° for positive fields and 270° for negative fields. The possible states are sketched below, with the black curved line representing the contacted region of the disk where the magnetic state is probed. a) When two small jumps are found for low external fields the chirality of the nucleated vortex is clockwise for negative fields and counter-clockwise for positive fields. b) When two large jumps are found for low external fields the chirality of the vortex must be counterclockwise for negative fields and clockwise for positive fields. c) When a large jump is found first for negative fields and a small jump first for positive fields, the chirality of the vortex can be determined as counterclockwise for both cases. d) When a large jump is found for first for positive fields a small jump first for negative fields the vortex chirality is clockwise for both cases.

region completely reverses, corresponding to a large change in the signal at high reverse fields. Returning to positive fields a small jump is first seen (III-IV). In this case this means that the top of the disk remains largely oriented to the left and a counter-clockwise vortex has been nucleated. This is then switched back to the original state at high fields (IV-I) with a large jump in the signal as the magnetization in the top of the disk reverses direction. With the same logic we can consider the other possible chiralities of the system as shown in (b)-(d), where it can be seen that the chirality of the vortex can be directly inferred from the relative size of the jumps - i.e. whether the small jump occurs at a small field or a large field for a given field direction.

As mentioned before, the more complicated behaviour in the experimental system can be attributed to the presence of defects as well as small changes to the quasi-uniform and vortex state that occur depending on the size of the field. Furthermore, for varying angles of the field and depending on the exact region of vortex core expulsion and annihilation, the relative size of the different jumps corresponding to the two processes would also be expected to change. Since the size of the signal is ultimately determined by the relative alignment of the absorbing magnetization with the spin current direction, it is the relative size of changes to the magnetization with respect to this axis that is important in deciding the size of the jump. Nevertheless, when taking these additional factors into account the simple model can describe the experimental behaviour well, in particular explaining the very different sizes of the observed jumps in the signal for the largely two-step switching events in Figure 3.

C. First Order Reversal Curves

To quantitatively test the model in detail we perform first order reversal curve (FORC) analysis[60,61] to test the stability of the state and check the size of the expected signals. The results for the case of the 351/171° field axis with positive pulses in the left electrode of density 7.6×10^{11} Am^{-2} are presented in Figure 6. The complete hysteresis curve as presented in the previous measurements is shown in (a). Note that the absolute size of the signal is different from that for the equivalent measurement shown previously in Figure 3 d (ii) which was performed at a different time. This is due to a different zero offset, which can arise from vari-

ous sources such as thermal effects.[62,63] Importantly the symmetry, shape and relative size of the signal changes are consistent between the different measurements, indicative of consistent behaviour. For the FORC analysis we start from the saturated state at positive fields (I) and we reduce the field until we see the first jump in the signal at a negative field around -10 mT, as shown in (b), at which point we are in state IIa. We then reduce the field to zero again and measure the signal at remanence to check the state of the system after this jump (II). As shown in (c) we then perform a measurement where we continue with the hysteresis loop to negative saturation (III) and back to positive fields again until the signal jumps around +10 mT (IVa), at which point we again reduce the field to zero to check the state of the system after the first positive jump (IV).

As previously determined, the magnetization direction of the left injector, which defines the polarization direction of the injected spin current, is 135°. The non-local signal then probes the relative angle between the spin current and the detector magnetization in the absorbed region, θ. In state I we have the monodomain state with the magnetization of the disk expected to be aligned with the external field at 351°, hence the expected angle between the magnetization and spin current is 141°. From the relative size of the signal we can calculate the experimental angle between the spin current and magnetization, since $V_{NL} \propto \cos\theta$.[64] This yields $\theta_I = 144 \pm 1°$, in good agreement with the expected value of $\theta_I = 141°$, in particular if we take into account the likelihood of a small canting of the magnetization at the edges of the disk in the quasi-uniform state.[10] Following the first jump in the signal to state IIa we find the angle between the spin current and the magnetization to be $\theta_{IIa} = 123 \pm 1°$. This indicates the magnetization in the absorbed region is directed in the $258 \pm 1°$ axis, consistent with the vortex state nucleation occurring via a buckled state or an off-centred vortex core.[59] This state then forms a stable state at zero field (II), with $\theta_{II} = 133 \pm 1°$ and $M2$ along $268 \pm 1°$, consistent with the expectation of 270° for the top

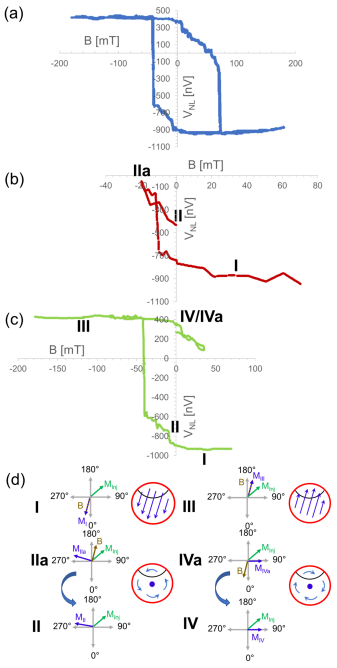

FIG. 6. First Order Reversal Curve (FORC) analysis for the 351/171° field axis with positive pulses in the left electrode of density 7.6×10^{11} Am^{-2}. (a) presents the full hysteresis loop of the system with 4 main jumps in the signal. (b) presents the portion of the minor loop from positive saturation, down past the first negative jump at ∼-10 mT and back to zero. (c) Presents the partial loop where the measurement is performed until negative saturation and then the field is increased until the first positive field jump at +10 mT, after which the field is reduced to zero.The schematic representations of the different states are shown in (d), where the black curved line represents the contact region where the signal is probed. The angle of the magnetization in the relevant region (M_{I-IV}), positive field axis (B) and injector magnetization direction (M_{Inj}) are shown on the coordinates.

of the counter-clockwise vortex state. For state III we measure an angle of $\theta_{III} = 36 \pm 1°$ with $M3$ along $171 \pm 1°$, aligned with the field as expected. Then for states IV/IVa we measure $\theta_{IV,IVa} = 47 \pm 1°$ and M along $88 \pm 1°$, consistent with the expectation of $90 \pm 1°$ for the clockwise vortex state. These states and the rel-

evant angles of the field and magnetization are shown on the axes in (d).

Hence it can be seen that the FORC measurements provide quantitative agreement with the expected signals for the different states, directly revealing important details of the nucleation process and the stable configurations. Based on these result, as well as the simple model from before, we can re-examine the plots in Figure 3 in order to identify the different states. By considering the size of the signal and the relative angle of the magnetization with respect to the spin current axis, as indicated on the coordinates besides the plot, we schematically sketch the expected spin states in each case. In particular, the identification of the vortex state chirality is made possible based on this simple d.c. electrical measurement.

V. CONCLUSION

In summary we have studied the switching of a permalloy disk between quasi-uniform states and vortex states via fields and pure spin currents in a dual-injector non-local spin valve device. We find a modest influence of the pure spin current in affecting the switching fields when spin currents are injected from both the injector electrodes, which is possible with our device design. While the effect is small, with a measured field-current equivalence of only $(0.14 \pm 1) \times 10^{-15}$ Tm^2/A, the small overlap of the disk with the conduit and the low spin diffusion length in the ferromagnetic material mean that the action of the pure spin current is restricted to a small fraction of the total volume of the disk. Hence the potential efficiency of the pure spin current in affecting such magnetic states and switching is high. This approach of simultaneous application of spin currents with different orientation to switch the nanostructure could in the future also help to achieve faster switching by reducing the incubation time as compared to devices where collinear magnetization are used.

We are able to exploit the small probing region to extract details of the switching and magnetic states in the disk from a simple d.c. measurement scheme. In particular we are able to extract the chirality of the states from the relative size of the jumps in the hysteresis loop, as described by a simple model. Furthermore we find good quantitative agreement of the signal with these expected states by employing first order reversal curve analysis which confirms that the intermediate states during the switching are stable at remanence. This work highlights the versatility and strength of a suitably engineered non-local spin valve geometry in providing a detailed electrical probe of the magnetic states in a system as well as providing efficient means to manipulate those states.

ACKNOWLEDGEMENTS

We are very grateful to Dr. Herman Stoll for assistance with the development of the electrical measurement scheme employed in this work. We acknowledge financial support of the SFB/TRR 173 Spin+X: spin in its collective environment funded by the Deutsche Forschungsgemeinschaft (DFG, German Research Foundation) Project No. 290396061/TRR173 (in particular project B02), as well as the Graduate School of Excellence Materials Science in Mainz (No. GSC266). The devices were fabricated in the Plateforme Technologie Amont (PTA), for which support came from the French Renatech Network. Funding from the French ANR SOspin is acknowledged.

* klaeui@uni-mainz.de

[1] S. Bohlens, B. Krüger, A. Drews, M. Bolte, G. Meier, and D. Pfannkuche, "Current con-

trolled random-access memory based on magnetic vortex handedness," *Appl. Phys. Lett.*, vol. 93, no. 14, p. 142508, 2008.

[2] B. Pigeau, G. de Loubens, O. Klein, A. Riegler, F. Lochner, G. Schmidt, L. W. Molenkamp, V. S. Tiberkevich, and A. N. Slavin, "A frequency-controlled magnetic vortex memory," *Appl. Phys. Lett.*, vol. 96, no. 13, p. 132506, 2010.

[3] R. P. Cowburn, "Change of direction," *Nat. Mater.*, vol. 6, no. 4, pp. 255–256, 2007.

[4] G. Hrkac, P. S. Keatley, M. T. Bryan, and K. Butler, "Magnetic vortex oscillators," *J. Phys. D: Appl. Phys.*, vol. 48, no. 45, p. 453001, 2015.

[5] H. Jung, Y.-S. Choi, K.-S. Lee, D.-S. Han, Y.-S. Yu, M.-Y. Im, P. Fischer, and S.-K. Kim, "Logic operations based on magnetic-vortex-state networks," *ACS Nano*, vol. 6, no. 5, pp. 3712–3717, 2012.

[6] R. P. Cowburn, D. K. Koltsov, A. O. Adeyeye, M. E. Welland, and D. M. Tricker, "Single-domain circular nanomagnets," *Phys. Rev. Lett.*, vol. 83, pp. 1042–1045, 1999.

[7] R. P. Cowburn, "Property variation with shape in magnetic nanoelements," *J. Phys. D: Appl. Phys.*, vol. 33, no. 1, pp. R1–R16, 1999.

[8] K. Y. Guslienko and V. Novosad, "Vortex state stability in soft magnetic cylindrical nanodots," *J. Appl. Phys.*, vol. 96, no. 8, pp. 4451–4455, 2004.

[9] J. K. Ha, R. Hertel, and J. Kirschner, "Micromagnetic study of magnetic configurations in submicron permalloy disks," *Phys. Rev. B*, vol. 67, p. 224432, 2003.

[10] W. Scholz, K. Guslienko, V. Novosad, D. Suess, T. Schrefl, R. Chantrell, and J. Fidler, "Transition from single-domain to vortex state in soft magnetic cylindrical nanodots," *J. Magn. Magn. Mater.*, vol. 266, no. 1, pp. 155 – 163, 2003.

[11] C. A. F. Vaz, M. Kläui, L. J. Heyderman, C. David, F. Nolting, and J. A. C. Bland, "Multiplicity of magnetic domain states in circular elements probed by photoemission electron microscopy," *Phys. Rev. B*, vol. 72, p. 224426, 2005.

[12] T. Shinjo, T. Okuno, R. Hassdorf, †. K. Shigeto, and T. Ono, "Magnetic vortex core observation in circular dots of permalloy," *Science*, vol. 289, no. 5481, pp. 930–932, 2000.

[13] F. Junginger, M. Kläui, D. Backes, S. Krzyk, U. Rüdiger, T. Kasama, R. E. Dunin-Borkowski, J.-M. Feinberg, R. J. Harrison, and L. J. Heyderman, "Quantitative determination of vortex core dimensions in head-to-head domain walls using off-axis electron holography," *Appl. Phys. Lett.*, vol. 92, no. 11, p. 112502, 2008.

[14] K. Y. Guslienko, "Magnetic vortex state stability, reversal and dynamics in restricted geometries," *J. Nanosci. Nanotechnol.*, vol. 8, no. 6, p. 2745–2760, 2008.

[15] B. Van Waeyenberge, A. Puzic, H. Stoll, K. W. Chou, T. Tyliszczak, R. Hertel, M. Fähnle, H. Brückl, K. Rott, G. Reiss, I. Neudecker, D. Weiss, C. H. Back, and G. Schütz, "Magnetic vortex core reversal by excitation with short bursts of an alternating field," *Nature*, vol. 444, no. 7118, pp. 461–464, 2006.

[16] M. Cosset-Chéneau, L. Vila, G. Zahnd, D. Gusakova, V. T. Pham, C. Grèzes, X. Waintal, A. Marty, H. Jaffrès, and J.-P. Attané, "Measurement of the spin absorption anisotropy in lateral spin valves," arXiv:2007.14058, 2020.

[17] H. Stoll, M. Noske, M. Weigand, K. Richter, B. Krüger, R. M. Reeve, M. Hänze, C. F. Adolff, F.-U. Stein, G. Meier, M. Kläui, and G. Schütz, "Imaging spin dynamics on the nanoscale using x-ray microscopy," *Front. Phys.*, vol. 3, p. 26, 2015.

[18] R. P. Cowburn, D. K. Koltsov, A. O. Adeyeye, M. E. Welland, and D. M. Tricker, "Single-domain circular nanomagnets," *Phys. Rev. Lett.*, vol. 83, pp. 1042–1045, 1999.

[19] M. Goiriena-Goikoetxea, K. Y. Guslienko, M. Rouco, I. Orue, E. Berganza, M. Jaafar, A. Asenjo, M. L. Fernández-Gubieda, L. Fernández Barquín, and A. García-Arribas, "Magnetization reversal in circular vortex dots of small radius," *Nanoscale*, vol. 9, pp. 11269–11278, 2017.

[20] K. Y. Guslienko, V. Novosad, Y. Otani, H. Shima, and K. Fukamichi, "Magnetization reversal due to vortex nucleation, displacement, and annihilation in submicron ferromagnetic dot arrays," *Phys. Rev. B*, vol. 65, p. 024414, 2001.

[21] K.-M. Wu, J.-F. Wang, Y.-H. Wu, C.-M. Lee, J.-C. Wu, and L. Horng, "Vortex motion in magnetic disks with different geometric asymmetry," *J. Appl. Phys.*, vol. 103, no. 7, p. 07F314, 2008.

[22] T. Y. Chung and S. Y. Hsu, "Detection of the domain structure change using magnetotransport for a series of circular permalloy dots," *J. Appl. Phys.*, vol. 99, no. 8, p. 08B707, 2006.

[23] T. Wren and O. Kazakova, "Anisotropic magnetoresistance effect in sub-micron nickel disks," *J. Appl. Phys.*, vol. 117, no. 17, p. 17E134, 2015.

[24] P. Vavassori, M. Grimsditch, V. Metlushko, N. Zaluzec, and B. Ilic, "Magnetoresistance of

single magnetic vortices," *Appl. Phys. Lett.*, vol. 86, no. 7, p. 072507, 2005.

[25] J.-S. Kim, O. Boulle, S. Verstoep, L. Heyne, J. Rhensius, M. Kläui, L. J. Heyderman, F. Kronast, R. Mattheis, C. Ulysse, and G. Faini, "Current-induced vortex dynamics and pinning potentials probed by homodyne detection," *Phys. Rev. B*, vol. 82, p. 104427, 2010.

[26] M. Sushruth, J. P. Fried, A. Anane, S. Xavier, C. Deranlot, M. Kostylev, V. Cros, and P. J. Metaxas, "Electrical measurement of magnetic-field-impeded polarity switching of a ferromagnetic vortex core," *Phys. Rev. B*, vol. 94, p. 100402(R), 2016.

[27] A. Gangwar, H. G. Bauer, J.-Y. Chauleau, M. Noske, M. Weigand, H. Stoll, G. Schütz, and C. H. Back, "Electrical determination of vortex state in submicron magnetic elements," *Phys. Rev. B*, vol. 91, p. 094407, 2015.

[28] S. Kasai, Y. Nakatani, K. Kobayashi, H. Kohno, and T. Ono, "Current-driven resonant excitation of magnetic vortices," *Phys. Rev. Lett.*, vol. 97, p. 107204, 2006.

[29] M. Goto, H. Hata, A. Yamaguchi, Y. Nakatani, T. Yamaoka, Y. Nozaki, and H. Miyajima, "Electric spectroscopy of vortex states and dynamics in magnetic disks," *Phys. Rev. B*, vol. 84, p. 064406, 2011.

[30] P. Fischer, "X-ray imaging of magnetic structures," *IEEE Trans. Magn.*, vol. 51, no. 2, pp. 1–31, 2015.

[31] P. Krautscheid, R. M. Reeve, D. Schönke, I. Boventer, A. Conca, A. V. Chumak, B. Hillebrands, J. Ehrler, J. Osten, J. Fassbender, and M. Kläui, "Direct observation of spin diffusion enhanced nonadiabatic spin torque effects in rare-earth-doped permalloy," *Phys. Rev. B*, vol. 98, p. 214406, 2018.

[32] T. Pokhil, D. Song, and J. Nowak, "Spin vortex states and hysteretic properties of submicron size NiFe elements," *J. Appl. Phys.*, vol. 87, no. 9, pp. 6319–6321, 2000.

[33] F. J. Jedema, A. T. Filip, and B. J. van Wees, "Electrical spin injection and accumulation at room temperature in an all-metal mesoscopic spin valve," *Nature*, vol. 410, no. 6826, pp. 345–348, 2001.

[34] F. J. Jedema, M. S. Nijboer, A. T. Filip, and B. J. van Wees, "Spin injection and spin accumulation in all-metal mesoscopic spin valves," *Phys. Rev. B*, vol. 67, p. 085319, 2003.

[35] M. Johnson and R. H. Silsbee, "Interfacial charge-spin coupling: Injection and detection of spin magnetization in metals," *Phys. Rev. Lett.*, vol. 55, pp. 1790–1793, 1985.

[36] T. Kimura and Y. Otani, "Spin transport in lateral ferromagnetic/nonmagnetic hybrid structures," *J. Phys.: Condens. Matter*, vol. 19, no. 16, p. 165216, 2007.

[37] A. Pfeiffer, S. Hu, R. M. Reeve, A. Kronenberg, M. Jourdan, T. Kimura, and M. Kläui, "Spin currents injected electrically and thermally from highly spin polarized Co2MnSi," *Appl. Phys. Lett.*, vol. 107, no. 8, p. 082401, 2015.

[38] A. Pfeiffer, R. M. Reeve, and M. Kläui, "Importance of spin current generation and detection by spin injection and the spin hall effect for lateral spin valve performance," *J. Phys.: Condens. Matter*, vol. 30, no. 46, p. 465802, 2018.

[39] N. Kuhlmann, C. Swoboda, A. Vogel, T. Matsuyama, and G. Meier, "All-metal lateral spin valve operated by spin pumping," *Phys. Rev. B*, vol. 87, p. 104409, 2013.

[40] M. Yamada, D. Sato, N. Yoshida, M. Sato, K. Meguro, and S. Ogawa, "Scalability of spin accumulation sensor," *IEEE Trans. Magn.*, vol. 49, no. 2, pp. 713–717, 2013.

[41] Y. K. Takahashi, S. Kasai, S. Hirayama, S. Mitani, and K. Hono, "All-metallic lateral spin valves using Co2Fe(Ge0.5Ga0.5) heusler alloy with a large spin signal," *Appl. Phys. Lett.*, vol. 100, no. 5, p. 052405, 2012.

[42] Y. Xu, K. Xia, and Z. Ma, "Spin transfer torques in the nonlocal lateral spin valve," *Nanotechnology*, vol. 19, no. 23, p. 235404, 2008.

[43] A. Brataas, G. E. Bauer, and P. J. Kelly, "Non-collinear magnetoelectronics," *Phys. Rep.*, vol. 427, no. 4, pp. 157 – 255, 2006.

[44] T. Yang, T. Kimura, and Y. Otani, "Giant spin-accumulation signal and pure spin-current-induced reversible magnetization switching," *Nat. Phys.*, vol. 4, no. 11, pp. 851–854, 2008.

[45] T. Kimura, Y. Otani, and J. Hamrle, "Switching magnetization of a nanoscale ferromagnetic particle using nonlocal spin injection," *Phys. Rev. Lett.*, vol. 96, p. 037201, 2006.

[46] D. Ilgaz, J. Nievendick, L. Heyne, D. Backes, J. Rhensius, T. A. Moore, M. A. Niño, A. Locatelli, T. O. Menteş, A. v. Schmidsfeld, A. v. Bieren, S. Krzyk, L. J. Heyderman, and M. Kläui, "Domain-wall depinning assisted by pure spin currents," *Phys. Rev. Lett.*, vol. 105, p. 076601, 2010.

[47] N. Motzko, B. Burkhardt, N. Richter, R. Reeve, P. Laczkowski, W. Savero Torres, L. Vila, J.-

P. Attané, and M. Kläui, "Pure spin current-induced domain wall motion probed by localized spin signal detection," *Phys. Rev. B*, vol. 88, p. 214405, 2013.

[48] A. Pfeiffer, R. M. Reeve, M. Voto, W. Savero-Torres, N. Richter, L. Vila, J. P. Attané, L. Lopez-Diaz, and M. Kläui, "Geometrical control of pure spin current induced domain wall depinning," *J. Phys.: Condens. Matter*, vol. 29, no. 8, p. 085802, 2017.

[49] T. Kimura, Y. Otani, and J. Hamrle, "Determination of magnetic vortex chirality using lateral spin-valve geometry," *Applied Physics Letters*, vol. 87, no. 17, p. 172506, 2005.

[50] G. Zahnd, L. Vila, V. T. Pham, A. Marty, C. Beigné, C. Vergnaud, and J. P. Attané, "Giant magnetoresistance in lateral metallic nanostructures for spintronic applications," *Sci. Rep.*, vol. 7, no. 1, p. 9553, 2017.

[51] G. Zahnd, L. Vila, T. V. Pham, A. Marty, P. Laczkowski, W. S. Torres, C. Beigné, C. Vergnaud, M. Jamet, and J.-P. Attané, "Comparison of the use of NiFe and CoFe as electrodes for metallic lateral spin valves," *Nanotechnology*, vol. 27, no. 3, p. 035201, 2015.

[52] A. Pfeiffer, R. M. Reeve, K. Elphick, A. Hirohata, and M. Kläui, "Revealing the importance of interfaces for pure spin current transport," *Phys. Rev. Res.*, vol. 3, pp. 023110, 2021.

[53] S. Dubois, L. Piraux, J. M. George, K. Ounadjela, J. L. Duvail, and A. Fert, "Evidence for a short spin diffusion length in permalloy from the giant magnetoresistance of multilayered nanowires," *Phys. Rev. B*, vol. 60, pp. 477–484, 1999.

[54] S. Takahashi and S. Maekawa, "Spin injection and detection in magnetic nanostructures," *Phys. Rev. B*, vol. 67, p. 052409, 2003.

[55] W. S. Torres, A. Marty, P. Laczkowski, M. Jamet, L. Vila, and J.-P. Attané, "Calculation method of spin accumulations and spin signals in nanostructures using spin resistors," *Eur. Phys. J. B*, vol. 91, no. 2, p. 37, 2018.

[56] T. Kimura, T. Sato, and Y. Otani, "Temperature evolution of spin relaxation in a NiFe/Cu lateral spin valve," *Phys. Rev. Lett.*, vol. 100, p. 066602, 2008.

[57] E. Grimaldi, V. Krizakova, G. Sala, F. Yasin, S. Couet, G. Sankar Kar, K. Garello, and P. Gambardella, "Single-shot dynamics of spin–orbit torque and spin transfer torque switching in three-terminal magnetic tunnel junctions," *Nature Nanotechnol.*, vol. 15, pp. 111–117, Feb 2020.

[58] J. Heinen, O. Boulle, K. Rousseau, G. Malinowski, M. Kläui, H. J. M. Swagten, B. Koopmans, C. Ulysse, and G. Faini, "Current-induced domain wall motion in *co/pt* nanowires: Separating spin torque and oersted-field effects," *Appl. Phys. Lett.*, vol. 96, no. 20, p. 202510, 2010.

[59] M. Vaňatka, M. Urbánek, R. Jíra, L. Flajšman, M. Dhankhar, M.-Y. Im, J. Michalička, V. Uhlíř, and T. Šikola, "Magnetic vortex nucleation modes in static magnetic fields," *AIP Advances*, vol. 7, no. 10, p. 105103, 2017.

[60] I. D. Mayergoyz, *Mathematical models of hysteresis*. Springer, 2012.

[61] C. R. Pike, A. P. Roberts, and K. L. Verosub, "Characterizing interactions in fine magnetic particle systems using first order reversal curves," *J. Appl. Phys.*, vol. 85, no. 9, p. 6660–6667, 1999.

[62] S. Kasai, S. Hirayama, Y. K. Takahashi, S. Mitani, K. Hono, H. Adachi, J. Ieda, and S. Maekawa, "Thermal engineering of non-local resistance in lateral spin valves," *Appl. Phys. Lett.*, vol. 104, no. 16, p. 162410, 2014.

[63] M. Erekhinsky, F. Casanova, I. K. Schuller, and A. Sharoni, "Spin-dependent seebeck effect in non-local spin valve devices," *Appl. Phys. Lett.*, vol. 100, no. 21, p. 212401, 2012.

[64] T. Kimura, Y.C. Otani, and P. M. Levy, "Electrical control of the direction of spin accumulation," *Phys. Rev. Lett.*, vol. 99, p. 166601, 2007.